Study of Wind and PV Frequency Control in U.S. Power Grids – EI and TI Case Studies

Yong Liu, *Member, IEEE*, Shutang You, *Student Member, IEEE*, Yilu Liu, *Fellow, IEEE*

Abstract—**Renewable generations such as variable-speed wind and photovoltaic (PV) power plants have been expected to contribute to power systems' frequency response. This paper studies wind and PV power plants' frequency control in the U.S. Eastern Interconnection (EI) and Texas Interconnection (TI). Wide-area frequency measurement-validated EI and TI dynamic models and realistically-projected renewable distribution information make these two case studies much more practical than previous studies based on only small test system models. A set of wind and PV power plant frequency controls, such as inertia control and governor control, are employed. This paper serves as a practical guidance on how to implement wind and PV frequency controls in a bulk power system with a high renewable penetration.**

Index Terms—**Bulk power system, Frequency response, Wind power generation, PV, Governor Control, Inertia control.**

I. Introduction

AS two of the most promising renewable generations, wind and photovoltaic (PV) power plants have witnessed a dramatic growth in the past two decades. Many Giga Watts (GW)' wind and PV generation have been installed in countries such as the United States and China [1]. For smaller countries and their power grids, wind or PV generation may even be able to meet the majority of electricity demand at certain moments. For instance, on 7th January 2015, Ireland's wind generation peaked at 63% of its total load [2]. Not surprisingly, such a high level of renewable penetration poses a series of profound impacts on power system operation and control [3-5].

Lack of system inertia was identified as one example of renewable impacts [4, 6-8]. System inertia is closely related to power system's dynamic characteristics in many aspects and is a critical parameter of a bulk power grid. Taking power system frequency response as an example, grid frequency declines sharply in the first several seconds after losing a large power plant. Because of the intrinsic inertia, synchronous generators release their kinetic energy stored in the rotating mass into the grid, allowing governors to kick in for further frequency support. Besides the net power imbalance, the initial rate of change of frequency (ROCOF) is proportional to total system inertia, which determines the overall inertial response of synchronous generators. Since displacing synchronous generators

with wind and PV power plants will reduce the total system inertia, a power system's capability to arrest fast frequency declines may be jeopardized [9, 10].

Against this background, previous studies had developed different active power control strategies for wind and PV power plants in order to eliminate the potential negative impacts of renewables on bulk power system frequency response [11-20]. Regarding wind power plant inertia control, it takes advantage of the kinetic energy stored in wind blades and turbines and provides a synthetic inertial frequency response in seconds [11-16]. Wind power plants may still operate in the maximum power point tracking (MPPT) mode under normal operation conditions but because the kinetic energy has to be restored after the synthetic inertial response, this frequency control cannot be sustained for more than several seconds. Another type of frequency controls requires wind and PV power plants to reserve certain amount of power generation capacity as headroom and, consequently, some wind or PV power will be spilled during normal operations [21, 22].

Although a large number of conceptual designs exist, there were few studies that ever tested the proposed controls' effectiveness based on a measurement-validated bulk power system dynamic model and realistic renewable distribution information [17, 23]. That partially explains why system operators have been relatively slow in engaging wind and PV power plants in frequency control. Since the wind and PV frequency control will eventually be required as renewable penetration keeps increasing, it is necessary to implement and evaluate those controls on realistic bulk power system dynamic models. Therefore, this paper will use the U.S., Eastern Interconnection (EI) and Texas Interconnection (TI) as case studies, which serve as good examples of how frequency control can be implemented in bulk power systems.

The rest of this paper is organized as follows: Section II briefly introduces the EI and TI models and simulation scenarios; Section III demonstrates the potential impacts of lack of system inertia issue on EI and TI frequency responses; Section IV discusses the implementation and evaluation of renewable frequency control based on EI and TI models, and Section V concludes the whole paper.

Yong Liu, Shutang You, and Yilu Liu are all with Department of Electrical Engineering and Computer Science, the University of Tennessee, Knoxville, TN, 37996, USA. (E-mails: yliu66@utk.edu, syou3@vols.utk.edu, liu@utk.edu).

Yilu Liu is also with Oak Ridge National Laboratory, Oak Ridge, TN, 37831, USA.

II. Model Overview and Scenario Development

Two U.S. bulk power systems, EI and TI, will be used in this paper as case studies. In this section, these two power grids and their models/simulation scenarios will be described briefly.
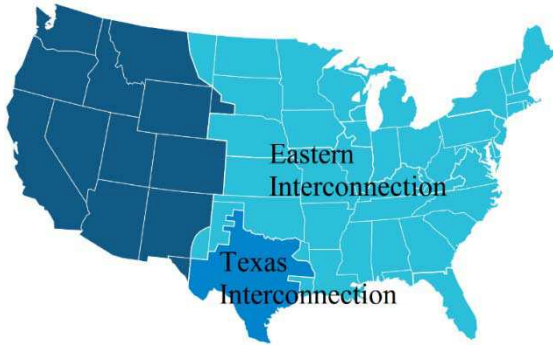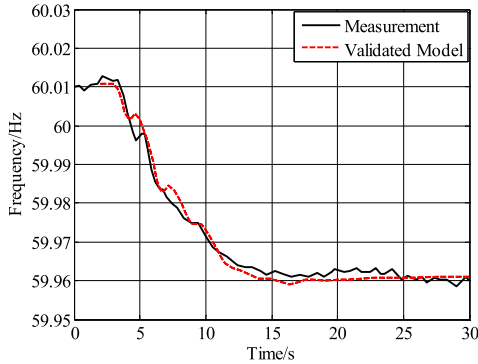
Fig. 1.   Geographic location of EI and TI

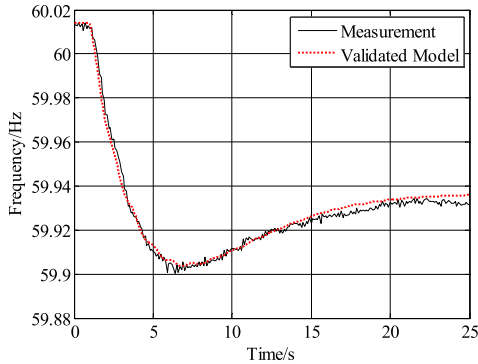Fig. 2.   Frequency response model validation in the EI

Fig. 3.   Frequency response model validation in the TI

A. EI and TI Overview

Fig. 1 shows the geographic locations of EI and TI in the United States. EI is one of the two major synchronized grids in the North America with an installed generation capacity of around 610 GW. It is the second largest power grid in the world [24]. Much smaller than EI, TI mainly covers the State of Texas and has about 74 GW for peak demand [25]. Both EI and TI have rich wind and solar resources in their territories although the resource distributions are quite different. Due to different system sizes and operation strategies etc., EI and TI own significantly different frequency characteristics [26-31]. An EI case study will provide valuable knowledge for the wind and PV frequency control in other power grids of similar sizes, such as continental Europe and China. Comparatively,
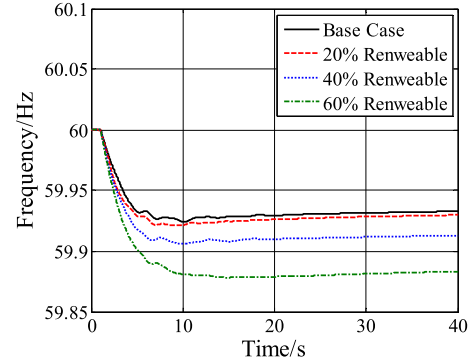

Fig. 4.   EI frequency response change due to renewable integration

TABLE I
BASIC INFORMATION OF EI AND TI MODELS

Statistic value	EI	TI
Total Bus Number	68309	6240
Generator Number	8337	690
Operating Generation Capacity	560 GW	76 GW
Load	540 GW	74 GW

TI serves as a great example for smaller power grids that exist in many other countries.

The EI multiregional modeling working group (MMWG) model was developed by the EI regional reliability councils and their member utilities and is the most detailed and realistic model for EI .()[32]. It is used for EI case study in this paper. Regarding TI, the 2015 summer peak model provided by Electric Reliability Council of Texas (ERCOT) is used in this paper. Some basic information of these two models are presented in Table I.

B. Model Validation Using Frequency Measurement

Wide area measurement systems (WAMS) have been deployed in both EI and TI and they provide high-resolution measurements of both systems' frequency responses [33-35]. Thanks to WAMS, it has been noticed that the EI frequency had been decreasing by 32% over 15 years before 2009 (1994-2009) [36]. It also revealed that the simulated frequency responses produced by original EI and TI models are more optimistic than WAMS measurements [37]. Therefore, in this section, the EI and TI dynamic models are tuned based on WAMS frequency measurements in order to enhance the model credibility.

As one of the model tuning measures, governor dead-band model [38, 39] was inserted to the original EI and TI models. Afterwards, spinning reserve and system inertia were adjusted coordinately to more realistic values. As a result, the simulated and measured frequency responses match each other to a much better extent in terms of ROCOF, nadir, and settling frequency. Multiple contingencies were used to verify the tuned model's credibility. One example of such contingencies is given in this subsection for EI and TI, as shown in Fig. 2 and Fig. 3, respectively.

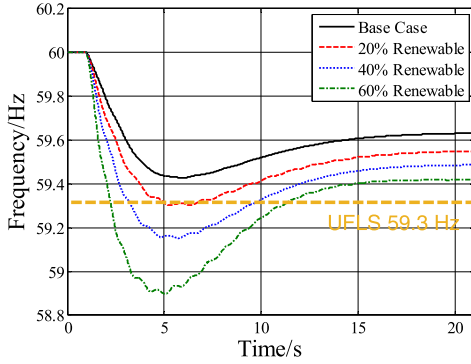As demonstrated by Fig. 2 and Fig. 3, the frequency

Fig. 5.   TI frequency response change due to renewable integration

TABLE II
WIND AND PV PENETRATION RATES IN EI AND TI SCENARIOS

Total renewable penetration	EI		TI	
	Wind	PV	Wind	PV
20%	15.6%	4.4%	14.7%	5.3%
40%	27.5%	12.5%	27.9%	12.1%
60%	36.6%	23.4%	37.4%	22.6%

responses of EI and TI produced by the tuned models show very good consistence with WAMS measurements and it lays a good foundation for later high renewable penetration studies. Additionally, the inter-area oscillations of the EI and TI models were also compared with the WAMS measurements, which results demonstrated that the models can represent the major features of the inter-area oscillation in the EI or TI.

C. Scenario Development

Different penetration levels of wind and PV are modeled in this paper's simulation scenarios. Additionally, renewable generation locations can influence system frequency response for a bulk power grid such as EI or TI. So it is beneficial to apply the realistic wind and PV generation geographic distribution in the case studies. In this section, the wind and PV distribution information from the U.S. Department of Energy Wind Vision Study was used to construct three simulation scenarios for either EI or TI [40]. The combined wind and PV penetration rates are chosen to be 20%, 40%, and 60%, respectively. As shown in Table II, wind generation has a larger share than PV in either EI or TI. The highest wind penetration rate is 36.6% for EI and 37.4% for TI while the highest PV penetration rate is 23.4% for EI and 22.6% for TI. All the wind generations are modeled as doubly-fed electric machines (DFIGs) since it is the most common wind power plant right now.

III. IMPACT OF RENEWABLE GENERATION ON FREQUENCY RESPONSE

Based on the scenarios developed in Section II, the impacts of wind and PV generations on the EI and TI frequency responses are evaluated in this section. The EI frequency response after a generation trip of 4,455 MW in each scenario is given in Fig. 4 and the frequency response metrics including

TABLE III
EI FREQUENCY RESPONSE METRICS CHANGE DUE TO RENEWABLE GENERATION

Frequency response metrics	Base case	20%	40%	60%
ROCOF (mHz/s)	23.2	26.6	32.4	37.2
Nadir (Hz)	59.924	59.921	59.906	59.878
Setting frequency (Hz)	59.933	59.930	59.913	59.883

TABLE IV
TI FREQUENCY RESPONSE METRICS CHANGE DUE TO RENEWABLE GENERATION

Frequency response metrics	Base case	20%	40%	60%
ROCOF (mHz/s)	220	280	400	650
Nadir (Hz)	59.43	59.31	59.16	58.91
Settling frequency (Hz)	59.63	59.55	59.49	59.42

ROCOF, nadir, and settling frequency are calculated in Table III.

In Fig. 4, even the EI base case does not have obvious governor response because of the governor dead band [38]. This "L-shaped" frequency response is typical for the EI system. As shown in Table III, ROCOF gets larger in the EI 20% scenario (26.6 mHz/s compared with 23.2 mHz/s) but nadir and setting frequency is only slightly influenced mostly because of the base case's weak governor response. For the EI 40% and 60% scenarios, ROCOF gets significantly larger and frequency nadir and settling frequency gets even lower. Specifically, ROCOF of the EI 60% scenario is about two times of that of the base case. However, different from ROCOF, the nadir change (from 59.924 Hz to 59.878 Hz) is not really dramatic at all. Since the first-stage under frequency load shedding (UFLS) for EI is set to be 59.5 Hz, the EI simulation results indicate that, it is unlikely for the EI system to trigger UFLS even at a renewable penetration rate up to 60%. This is mainly due to the extensive size of the EI system.

The TI frequency response after a generation disturbance of 2,760 MW in each scenario is given in Fig. 5 and the frequency metrics are presented in Table IV. As shown in Fig. 5 and Table IV, the TI frequency response declines dramatically with the increasing wind and PV penetration rates and this decline is much more significant than that of EI. Specifically, in the ERCOT 20% scenario, the TI frequency nadir declines to 59.31 Hz, which is very close to the TI first-stage UFLS threshold (59.3 Hz) [27, 41]. This indicates TI may need to take countermeasures to flight with the declining frequency response at a much lower renewable penetration rate than EI. This is obviously because TI is much smaller than EI. Please note that the fast load response at 59.7 Hz required by TI is not simulated in this study.

IV. WIND AND PV FREQUENCY CONTROL IN EI AND TI

In this section, the wind and PV frequency control schemes will be implemented and evaluated based on EI and TI dynamic models in order to eliminate the negative impacts of renewable penetration on frequency response and inter-area oscillations.
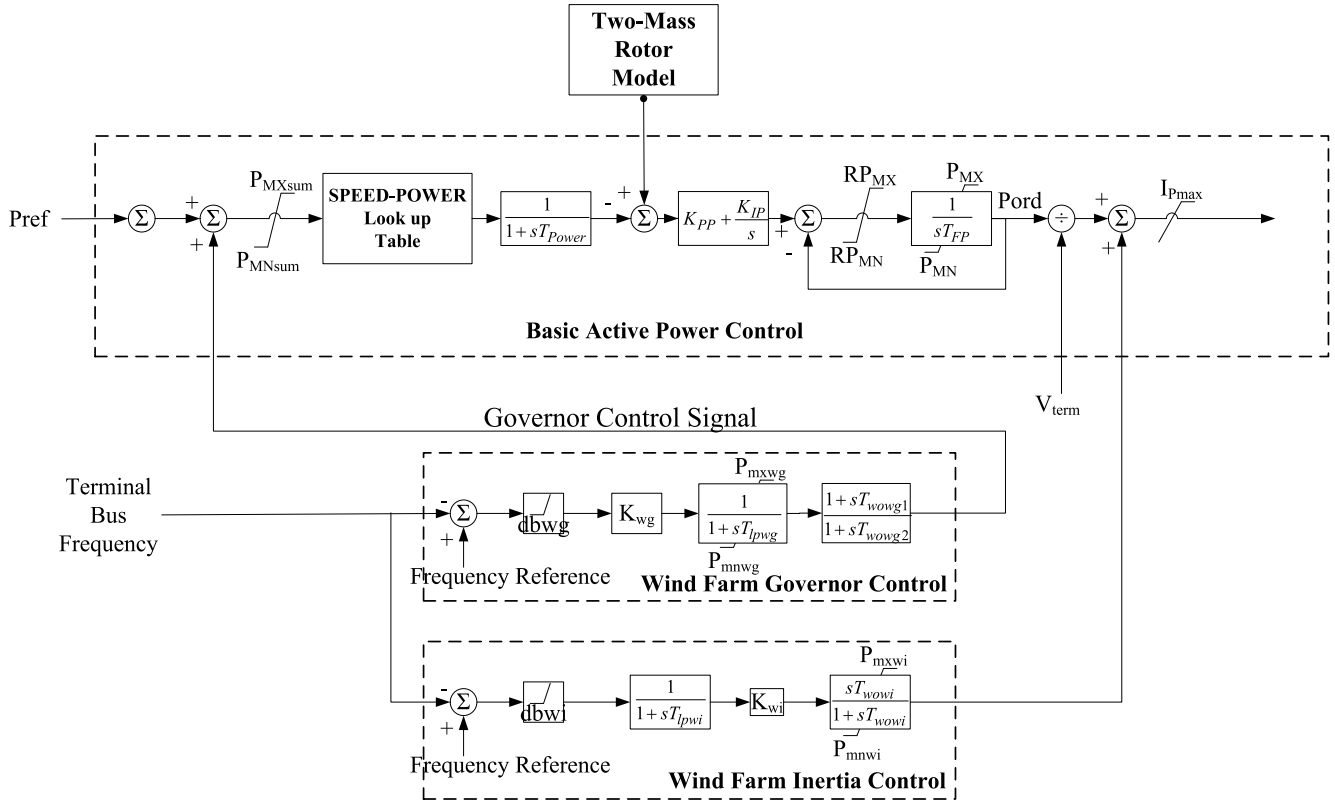
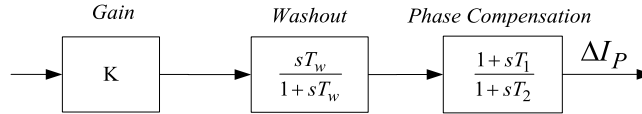Fig. 6. Diagram of wind farm active power control

Fig. 7. Wind farm oscillation damping control

A. Wind and PV Frequency Control

As mentioned in the Introduction, several different frequency controls have been proposed in the literature to enable wind and PV power plants to provide the synthetic inertial response. Thanks to its simplicity and robustness, droop-based inertia control is most likely to be applied in the industry first [42]. Therefore, this droop-based inertia control approach is implemented in this section.

Moreover, if a large portion of synchronous generators are displaced, the power system spinning reserve and governor response will also be reduced. As mentioned in [43], a wind turbine may reduce its rotational speed in order to release the reserved power generation capacity if it is working in the overspeed zone instead of MPPT. In this way, a synthetic "governor response" can be provided by wind power plants. Since wind generation is going to account for a significant portion of future EI and TI generation, this synthetic governor control is most likely to be required by the regulation agency for wind power plants. Therefore, a droop-based synthetic governor control is also implemented in this paper. The diagram of the wind power plant active power control is shown in Fig. 6. Dead bands have been used to avoid the excessive actions

of the synthetic inertia and governor controls caused by small random frequency variations during normal operation conditions. Filters are used to reject measurement noises or unwanted frequency components.

Because of the wind and PV power plants' capability to control active power in a fast manner, it also has huge potential to damp inter-area oscillations and contribute to the small-signal stability [42, 44]. A wind power plant oscillation damping controller similar to synchronous generator's power system stabilizer (PSS) is shown in Fig. 7. The signal washout block serves as a high-pass filter, with time constant T_w high enough to allow oscillation components of interests to pass. Either local or wide-area control signals can be used as the input to this oscillation damping controller, although wide-area control signals will be much more effective. Similar to wind power plants, PV power plants can also apply similar controls to provide governor response and oscillation damping effects. The synthetic governor and PSS control diagramS of PV power plants is shown in Fig. 8.
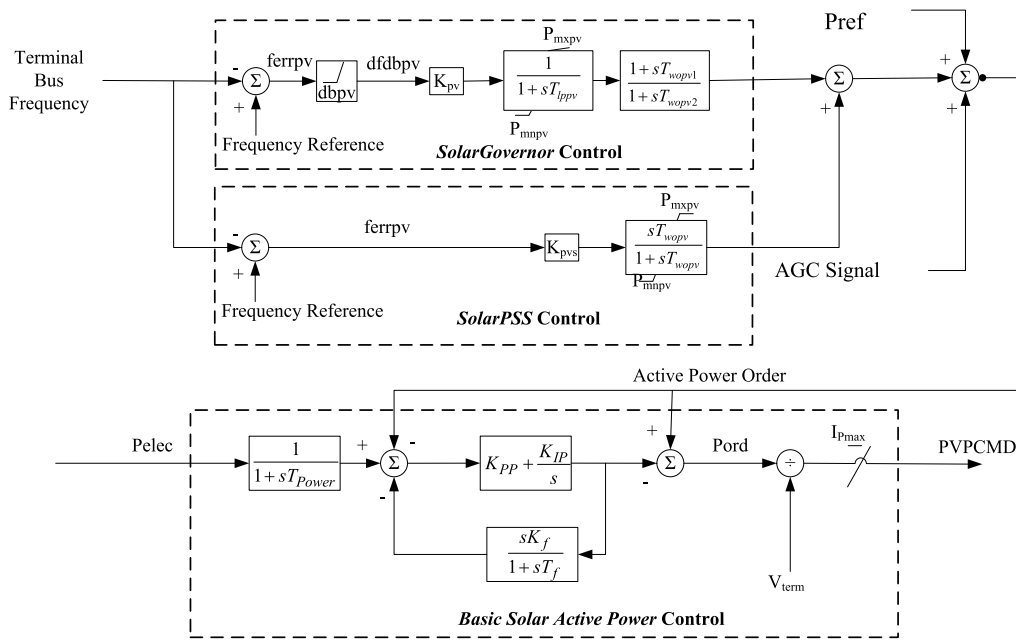
Fig. 8. Diagram of PV power plants active power control

B. EI and TI Frequency Response Improvement due to Wind and PV Frequency Control

As mentioned earlier, synthetic inertia control and governor control were implemented in the EI and TI wind and PV power plants. In this section, the effectiveness of these two controls on the EI and TI system frequency response will be discussed.

A 1 GW generation loss disturbance was simulated in EI. The active power outputs of a typical wind power plant with proposed frequency control functions are shown in Fig. 9 while the same wind power plant's wind turbine speed deviations are shown in Fig. 10. As shown by Fig. 9, inertia control enables wind power plants to increase their power outputs after a generation loss by use of the kinetic energy stored in wind turbines. However, this temporary active power surge cannot sustain for more than several seconds, which is followed by a "dip" of active power. This is due to the fact that the kinetic energy stored in wind turbines have to be "recharged" immediately, which leads to the "dip" of active power. This process can be obviously observed in Fig. 10. Due to inertia control, wind turbines reduce their rotation speeds to release the stored kinetic energy and then go back to its original rotation speed because of the "recharge" process. Moreover, Fig. 11 shows a typical PV plant's active power outputs with and without synthetic governor control while the EI system frequency responses with different control strategies are presented in Fig. 12. From Fig. 11, PV power plants contribute to frequency response by reserving some power generation capacity headroom. From Fig. 12, it can be seen that the wind power plants inertia control decreases the system ROCOF but the frequency nadir is even lower than that of the base case due to the "recharge" process. Therefore, wind power plant inertia control is not able to improve the EI system frequency response meaningfully on its own but it allows other
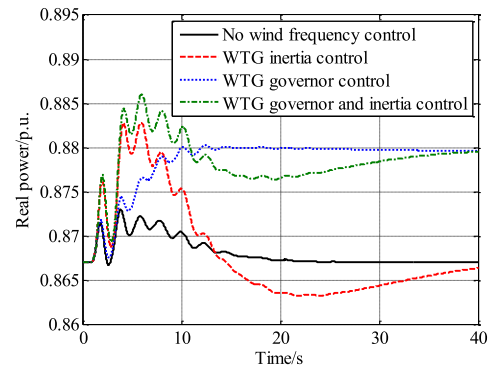

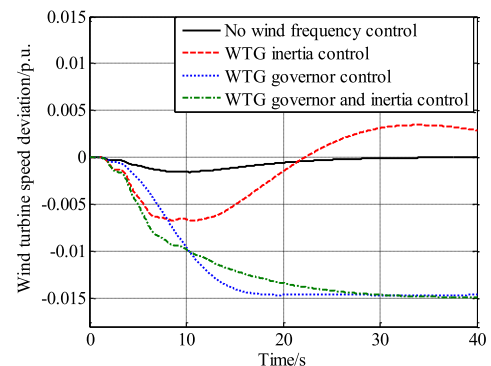Fig. 9. Active power output of a wind farm in the EI

Fig. 10. Wind turbine speed change of a wind farm in the EI

frequency controls (such as governor control) to have time to kick in before system frequency declines further.

As mentioned earlier, since some power generation capacity can be reserved by over-speeding, wind power plant governor
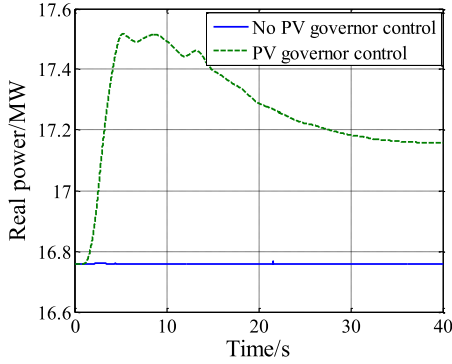
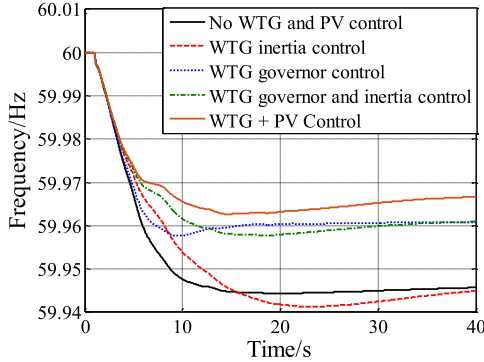Fig. 11. Active power output of a PV power plant in the EI

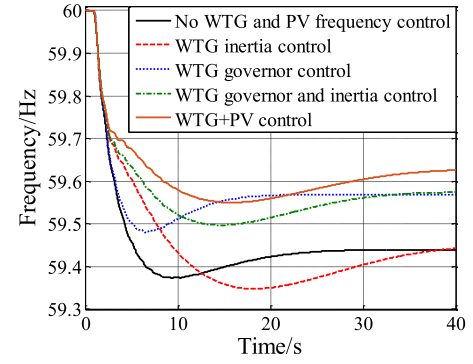Fig. 13. TI frequency response improvement with wind farm and PV controls

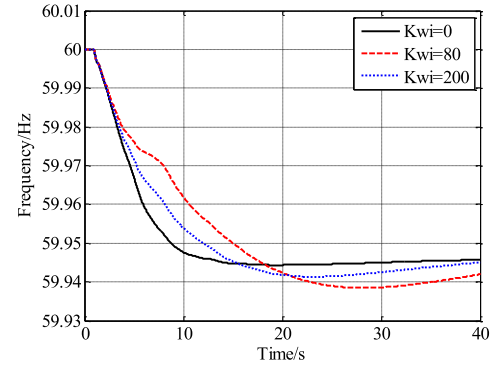Fig. 12. EI frequency response improvement with wind farm and PV controls

Fig. 14. K_{wi} value change impact on frequency response

control can be achieved by decreasing the wind turbine speed to release the reserved capacity. Unlike wind power plant inertia control, the increased wind power plant power output by wind power plant governor control can sustain, as shown in Fig. 9 and Fig. 10. Fig. 12 demonstrates that the governor control helps reduce both frequency nadir and settling frequency but not ROCOF. Apparently, wind power plant inertia control can mainly reduce ROCOF and governor control is able to decrease frequency nadir and settling frequency, therefore, a combination of inertia and governor controls can enhance the EI system frequency response much more effectively. As shown in Fig. 12, employing these controls simultaneously reduces both the ROCOF and frequency nadir. However, in order to bring the frequency back to its nominal value (60 Hz for U.S.), automatic generation control (AGC) have to be employed.

Similar to the EI study, the wind power plant inertia control mostly improves the TI ROCOF and governor control reduces the frequency nadir and settling frequency, as presented in Fig. 13. Obviously, it requires inertia and governor control to work together to be able to improve the TI frequency response in terms of multiple metrics.

C. Parameter Tuning

It is understandable that inertia control gain K_{wi} and governor control gain (K_{wg} and K_{pv}) are the main parameters that determine the control effectiveness. A control parameter sensitivity study is first given in this subsection. Fig. 14 shows

that ROCOF will benefit from a larger K_{wi} but the frequency nadir will suffer. Furthermore, it is worth noting that the wind turbines may stall if too much kinetic energy is exploited and the turbine speeds fall too low. Comparatively, a steeper governor droop (larger K_{wg} and K_{pv}) reduces the frequency nadir further as long as sufficient power generation capacity is reserved, as shown in Fig. 15. Apparently, appropriate parameter setting is crucial for wind and PV frequency controls, especially in a large power system with high amounts of renewables.

There may be thousands of wind and PV power plants in a large power system such as EI and TI. More importantly, wind and solar resources are usually fast changing. Therefore, a perfect parameter optimization solution for such a large number of renewable power plants will be almost impossible to obtain. In this subsection, from the engineering point of view, a practical way to tune those parameters will be developed. To solve this problem, a statistical analysis of the EI generators' inertia values was conducted, which results are given in Fig. 16.

As shown in Fig. 16, the average generator inertia value in the EI is around 3.9s per 100 MW. This average inertia value can be used as a guideline to tune the K_{wi} values of wind power plants inertia controls in the EI system. For example, in order not to decrease system inertia by displacing a 300 MW synchronous generation with wind power plants, the installed wind power plants inertia control K_{wi} value should be tuned to provide a synthetic inertia equivalent to 300 MW $*$ 3.9s/100 MW=11.7s. As a result, the overall system inertia
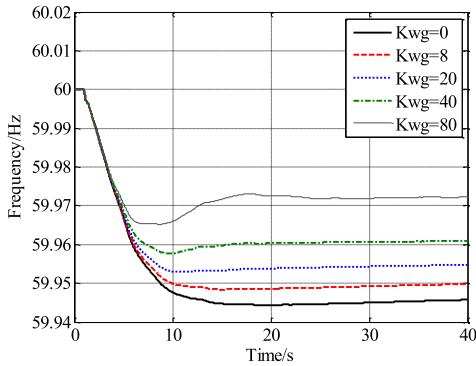
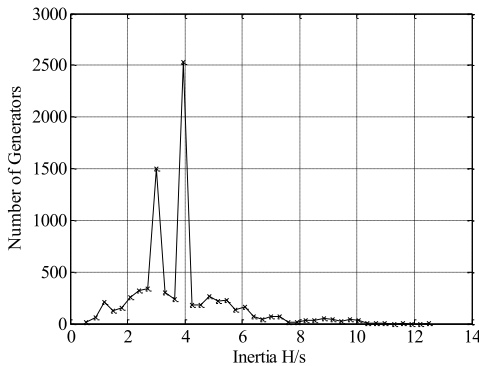Fig. 15. K$_{wg}$ value change impact on frequency response

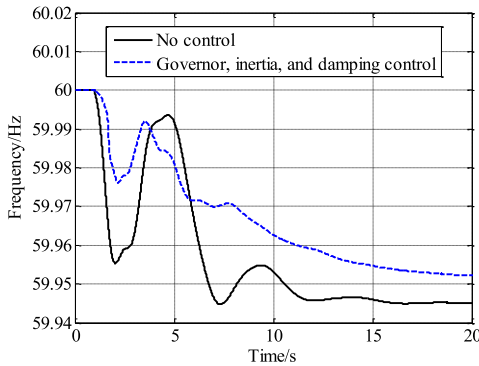Fig. 16. EI generator inertia value distribution

Fig. 17. Frequency of a 500kV Bus in EI due to simultaneous frequency control and oscillation damping

won't be decreased. Actually, since a variable-speed wind turbine has more kinetic energy stored than a synchronous generator of equivalent power generation capacity, providing a synthetic inertia equivalent to that of synchronous generator will not be an issue for wind turbines at all. However, though the overall system inertia value is not decreased because of the wind power plant inertia control, the system inertia geographic distribution may be changed since wind power plants may not be in the same location as the synchronous generations. This inertia geographic change will not influence the system average frequency response but may have more obvious impacts on inter-area oscillations.

Regarding wind and PV governor control, since the gov-

ernor droop gain is uniformly chosen to be 20 (1/R=1/0.05) for all synchronous generators in the EI, the same value can be used for EI wind and PV power plants. Furthermore, the dead-band of these governor controls should be similar or even smaller than governor dead-band of synchronous generators (currently 36 mHz for generators larger than 400 MW in EI).

D. Electromechanical Oscillation Damping

Synthetic inertia and governor controls provided by wind and PV have been demonstrated in previous subsections to be able to improve both EI and TI's frequency response. This active power control capability can also be utilized to damp inter-area oscillations. Fig. 17 shows the frequency of a 500 kV bus in EI, which includes an obvious oscillation component. With the comprehensive controls including damping control, the frequency response has been improved and oscillations has been damped effectively. This case study demonstrates the potential of renewable power plants to improve power system stability.

V. CONCLUSION

In this paper, wind and PV frequency controls were implemented based on the EI and TI measurement-validated system models and realistic renewable penetration information. Simulation results showed that synthetic inertia and governor control provided by wind and PV power plants are able to mitigate the negative effects of increasing renewable penetration levels on EI and TI's frequency responses. Most importantly, a practical approach of tuning the synthetic inertia and governor control parameters was introduced. These two case studies can serve as good examples for the future renewable integration studies in bulk power systems.

REFERENCES

[1] G. W. S. GWEC, "Global wind energy council," ed: February, 2013.
[2] "The Future Role of Wind in Ireland's Energy Mix - Irish On-shore Wind in Numbers," in Engineers Ireland Conference, 2015, p. 12.
[3] S. You, G. Kou, Y. Liu, X. Zhang, Y. Cui, M. J. Till, et al., "Impact of High PV Penetration on the Inter-Area Oscillations in the US Eastern Interconnection," IEEE Access, vol. 5, pp. 4361-4369, 2017.
[4] S. You, X. Zhang, L. Yong, Y. Su, Y. Liu, and S. Hadley, "Impact of high PV penetration on US eastern interconnection frequency response," in Proc. Power Energy Soc. General Meeting (PESGM), 2017, pp. 1-5.
[5] J. Kabouris and F. D. Kanellos, "Impacts of Large-Scale Wind Penetration on Designing and Operation of Electric Power Systems," IEEE Transactions on Sustainable Energy, vol. 1, pp. 107-114, 2010.
[6] N. Miller, C. Loutan, M. Shao, and K. Clark, "Emergency response: US system frequency with high wind penetration," IEEE Power and Energy Magazine, vol. 11, pp. 63-71, 2013.
[7] Y. Zhang, V. Gevorgian, E. Ela, V. Singhvi, and P. Pourbeik, "Role of wind power in primary frequency response of an interconnection," National Renewable Energy Laboratory (NREL), Golden, CO, USA, 2013.
[8] S. You, Y. Liu, G. Kou, X. Zhang, W. Yao, Y. Su, et al., "Non-Invasive Identification of Inertia Distribution Change in High Renewable Systems Using Distribution Level PMU," IEEE Transactions on Power Systems, 2017.

[9] J. Tan, Y. Zhang, I. Krad, V. Gevorgian, and E. Ela, "Investigating Power System Primary and Secondary Reserve Interaction under High Wind Power Penetration Using Frequency Response Model," in Grid of the Future Symposium, Chicago, 2015.

[10] J. Tan and Y. Zhang, "Coordinated Control Strategy of a Battery Energy Storage System to Support a Wind Power Plant Providing Multi-Timescale Frequency Ancillary Services," IEEE Transactions on Sustainable Energy, 2017.

[11] M. F. M. Arani and E. F. El-Saadany, "Implementing virtual inertia in DFIG-based wind power generation," IEEE Transactions on Power Systems, vol. 28, pp. 1373-1384, 2013.

[12] J. Morren, S. W. De Haan, W. L. Kling, and J. Ferreira, "Wind turbines emulating inertia and supporting primary frequency control," IEEE Transactions on power systems, vol. 21, pp. 433-434, 2006.

[13] G. Lalor, A. Mullane, and M. O'Malley, "Frequency control and wind turbine technologies," IEEE Transactions on Power Systems, vol. 20, pp. 1905-1913, 2005.

[14] P.-K. Keung, P. Li, H. Banakar, and B. T. Ooi, "Kinetic energy of wind-turbine generators for system frequency support," IEEE Transactions on Power Systems, vol. 24, pp. 279-287, 2009.

[15] M. Kayıkçi and J. V. Milanovic, "Dynamic contribution of DFIG-based wind plants to system frequency disturbances," IEEE Transactions on Power Systems, vol. 24, pp. 859-867, 2009.

[16] L. Ruttledge, N. W. Miller, J. O'Sullivan, and D. Flynn, "Frequency response of power systems with variable speed wind turbines," IEEE transactions on Sustainable Energy, vol. 3, pp. 683-691, 2012.

[17] V. Gevorgian, Y. Zhang, and E. Ela, "Investigating the impacts of wind generation participation in interconnection frequency response," IEEE transactions on Sustainable Energy, vol. 6, pp. 1004-1012, 2015.

[18] N. Miller, K. Clark, and M. Shao, "Frequency responsive wind plant controls: Impacts on grid performance," in Power and Energy Society General Meeting, 2011 IEEE, 2011, pp. 1-8.

[19] N. Miller, R. Delmerico, K. Kuruvilla, and M. Shao, "Frequency responsive controls for wind plants in grids with wind high penetration," in Power and Energy Society General Meeting, 2012 IEEE, 2012, pp. 1-7.

[20] F. Wilches-Bernal, J. H. Chow, and J. J. Sanchez-Gasca, "A Fundamental Study of Applying Wind Turbines for Power System Frequency Control," IEEE Transactions on Power Systems, vol. 31, pp. 1496-1505, 2016.

[21] A. Tuohy, P. Meibom, E. Denny, and M. O'Malley, "Unit commitment for systems with significant wind penetration," IEEE Transactions on Power Systems, vol. 24, pp. 592-601, 2009.

[22] Y. V. Makarov, C. Loutan, J. Ma, and P. De Mello, "Operational impacts of wind generation on California power systems," IEEE Transactions on Power Systems, vol. 24, pp. 1039-1050, 2009.

[23] N. Miller, M. Shao, S. Venkataraman, C. Loutan, and M. Rothleder, "Frequency response of California and WECC under high wind and solar conditions," in Power and Energy Society General Meeting, 2012 IEEE, 2012, pp. 1-8.

[24] N. Miller, M. Shao, S. Pajic, and R. D'Aquila, "Eastern frequency response study," Contract, vol. 303, pp. 275-3000, 2013.

[25] M. Majidi-Qadikolai and R. Baldick, "Integration of $ N-1$ Contingency Analysis With Systematic Transmission Capacity Expansion Planning: ERCOT Case Study," IEEE Transactions on Power Systems, vol. 31, pp. 2234-2245, 2016.

[26] M. Lauby, J. Bian, S. Ekisheva, and M. Varghese, "Eastern interconnection frequency response trends," in Power and Energy Society General Meeting (PES), 2013 IEEE, 2013, pp. 1-5.

[27] J. W. Ingleson and E. Allen, "Tracking the eastern interconnection frequency governing characteristic," in Power and Energy Society General Meeting, 2010 IEEE, 2010, pp. 1-6.

[28] P. Mackin, "Dynamic simulation studies of the frequency response of the three US interconnections with increased wind generation," Lawrence Berkeley National Laboratory, 2011.

[29] S. Sharma, S.-H. Huang, and N. Sarma, "System inertial frequency response estimation and impact of renewable resources in ERCOT interconnection," in Power and Energy Society General Meeting, 2011 IEEE, 2011, pp. 1-6.

[30] H. Chavez, R. Baldick, and S. Sharma, "Regulation adequacy analysis under high wind penetration scenarios in ERCOT nodal," IEEE Transactions on Sustainable Energy, vol. 3, pp. 743-750, 2012.

[31] M. Lauby, J. Bian, S. Ekisheva, and M. Varghese, "Frequency response assessment of ERCOT and Québec Interconnections," in North American Power Symposium (NAPS), 2014, 2014, pp. 1-5.

[32] N. W. Miller, M. Shao, R. D'aquila, S. Pajic, and K. Clark, "Frequency Response of the US Eastern Interconnection under Conditions of High Wind and Solar Generation," in Green Technologies Conference (GreenTech), 2015 Seventh Annual IEEE, 2015, pp. 21-28.

[33] Y. Liu, L. Zhan, Y. Zhang, P. N. Markham, D. Zhou, J. Guo, et al., "Wide-area-measurement system development at the distribution level: an FNET/GridEye example," IEEE Transactions on Power Delivery, vol. 31, pp. 721-731, 2016.

[34] Y. Liu, W. Yao, D. Zhou, L. Wu, S. You, H. Liu, et al., "Recent developments of FNET/GridEye—A situational awareness tool for smart grid," CSEE Journal of Power and Energy Systems, vol. 2, pp. 19-27, 2016.

[35] Y. Liu, S. You, W. Yao, Y. Cui, L. Wu, D. Zhou, et al., "A Distribution Level Wide Area Monitoring System for the Electric Power Grid–FNET/GridEye," IEEE Access, vol. 5, pp. 2329-2338, 2017.

[36] N. Subcommittee, "ALR1-12 interconnection frequency response," http://www.nerc.com/pa/RAPA/ri/Pages/InterconnectionFrequency Response.aspx, 2015.

[37] L. Chen, "Wide-area measurement application and power system dynamics," 2011.

[38] G. Kou, P. Markham, S. Hadley, T. King, and Y. Liu, "Impact of governor deadband on frequency response of the US Eastern Interconnection," IEEE Transactions on Smart Grid, vol. 7, pp. 1368-1377, 2016.

[39] S. Mohajeryami, A. R. Neelakantan, I. N. Moghaddam, and Z. Salami, "Modeling of deadband function of governor model and its effect on frequency Response characteristics," in North American Power Symposium (NAPS), 2015, 2015, pp. 1-5.

[40] W. Vision, "A New Era for Wind Power in the United States," Technical report, US Department of Energy, Washington, DC2015.

[41] ERCOT, "Under frequency load shedding," 2006.

[42] J. Van de Vyver, J. D. De Kooning, B. Meersman, L. Vandevelde, and T. L. Vandoorn, "Droop control as an alternative inertial response strategy for the synthetic inertia on wind turbines," IEEE Transactions on Power Systems, vol. 31, pp. 1129-1138, 2016.

[43] G. Ramtharan, N. Jenkins, and J. Ekanayake, "Frequency support from doubly fed induction generator wind turbines," IET Renewable Power Generation, vol. 1, pp. 3-9, 2007.

[44] G. Tsourakis, B. M. Nomikos, and C. D. Vournas, "Contribution of doubly fed wind generators to oscillation damping," IEEE Transactions on energy conversion, vol. 24, pp. 783-791, 2009.

Yong Liu (S'10-M'15) is currently a research assistant preofessor in the Department of Electrical Engineering and Computer Science at the University of Tennessee, Knoxville. He is also a member of the DOE/NSF-cofunded engineering research center CURENT. He received his B.S. and M.S. degree of Electrical Engineering from Shandong University in 2007 and 2010 respectively and obtained his Ph.D. degree from University of Tennessee, Knoxville, in 2013. His research interests include power system wide-area measurement, renewable energy integration, and power system dynamic modeling and analysis.
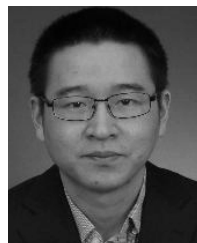
Shutang You (S'13) received the B.S. degree in Electrical Engineering in 2011, and the M.S. degree in Electrical Engineering in 2014 at Xi'an Jiaotong University, China. He is currently working towards his Ph.D. degree in the Power IT lab at the University of Tennessee, Knoxville, TN, USA. His research interests include power grid dynamics modelling and monitoring, system operation simulation and expansion planning, as well as the application of signal processing techniques in power grids.

Yilu Liu (S'88–M'89–SM'99–F'04) is currently the Governor's Chair at the University of Tennessee, Knoxville and Oak Ridge National Laboratory. Prior to joining UTK/ORNL, she was a Professor at Virginia Tech. She is a member of the U.S. National Academy of Engineering. She received her M.S. and Ph.D. degrees from the Ohio State University, Columbus, in 1986 and 1989. She received the B.S. degree from Xian Jiaotong University. She led the effort to create the North American power grid Frequency Monitoring Network (FNET) at Virginia Tech, which is now operated at UTK and ORNL as GridEye. Her current research interests include power system wide-area monitoring and control, large interconnection-level dynamic simulations, electromagnetic transient analysis, and power transformer modeling and diagnosis. (liu@utk.edu)